

# Difference frequency generation of 8- $\mu\text{m}$ radiation in orientation-patterned GaAs

O. Levi, T. J. Pinguet, T. Skauli, L. A. Eyres, K. R. Parameswaran, J. S. Harris, Jr., and M. M. Fejer

*E. L. Ginzton Laboratory, Stanford University, Stanford, California 94305*

T. J. Kulp and S. E. Bisson

*Diagnostics and Remote Sensing Department, Sandia National Laboratories, P.O. Box 969, MS 9051, Livermore, California 94551-0969*

B. Gerard, E. Lallier, and L. Becouarn

*Laboratoire Central de Recherche, Thales, Domaine de Corbeville-91404, Orsay Cedex, France*

Received May 20, 2002

First-order quasi-phase-matched difference frequency generation of narrowband tunable mid-infrared light is demonstrated in orientation-patterned GaAs. The all-epitaxial orientation-patterned crystal is fabricated by a combination of molecular beam epitaxy and hydride vapor phase epitaxy. Lasers at 1.3 and 1.55  $\mu\text{m}$  were mixed to give an idler output at 8  $\mu\text{m}$ , with power and wavelength tuning consistent with theoretical estimates, indicating excellent material uniformity over the 19-mm-long and 500- $\mu\text{m}$ -thick device. © 2002 Optical Society of America

OCIS codes: 190.2620, 190.4360, 190.4400, 190.4720, 190.5970.

Tunable mid-IR radiation is useful in applications such as spectroscopy,<sup>1</sup> remote sensing, and IR countermeasures. Devices based on nonlinear frequency conversion are often used to generate suitable coherent radiation. For applications such as IR countermeasures that demand efficient generation of high peak or average output powers, optical parametric oscillators are usually the preferred devices. Difference frequency generation (DFG), although it is less efficient, often provides a simpler method to transfer the narrow linewidth and frequency stability of the pump lasers to the mid-IR output and so is often attractive for precision spectroscopic applications. Nonlinear materials combining large nonlinear coefficients, noncritical phase matching, and means for phase matching over a broad spectral range are essential for meeting the demanding requirements of high-efficiency DFG interactions. Here we report on the use of a recently developed material for quasi-phase-matched (QPM) nonlinear optics, orientation-patterned (OP) GaAs, for converting near-IR source into the 8- $\mu\text{m}$  band for mid-IR spectroscopic applications. The wavelength-tuning curve and idler power are measured and found to be consistent with theoretical predictions, indicating that the OP GaAs material quality is good.

GaAs is an attractive material for mid-IR nonlinear optics, as it has a wide transparency range, 0.9–17  $\mu\text{m}$ , low absorption, high thermal conductivity, and large nonlinear susceptibility ( $d_{14} \geq 90$  pm/V for GaAs) but lacks birefringence and so requires an alternative such as quasi-phase matching. Previous GaAs QPM devices based on diffusion bonding of thin wafers<sup>2,3</sup> presented challenging fabrication tolerances and were difficult to extend to short coherence lengths. Waveguide QPM devices with periodic monolithic switching between GaAs/Al<sub>x</sub>Ga<sub>1-x</sub>As layers result in reduced effective nonlinearity.<sup>4</sup> Recently, a method was developed for all-epitaxial wafer-scale fabrication of thick OP GaAs templates by a combination of molecu-

lar beam epitaxy and hydride vapor phase epitaxy (HVPE).<sup>5,6</sup> DFG was previously demonstrated with diffusion-bonded GaAs devices and third-order QPM interaction.<sup>7,8</sup> In comparison, we obtained OP GaAs devices of good quality with domain widths as low as 7.7  $\mu\text{m}$ , thus allowing a wide range of first-order QPM DFG interaction with inherently higher conversion efficiencies.<sup>9</sup>

The efficiency of an optimally focused DFG interaction can be written as<sup>7,10</sup>

$$P_{\text{out}}(L) = \eta_0 L P_{\text{pump}} P_{\text{signal}}(0),$$

where  $L$  is the length of the crystal,  $P_{\text{pump}}$  and  $P_{\text{signal}}$  are the powers of the two input lasers (pump and signal, respectively), and the normalized efficiency  $\eta_0$  [ $\text{W}^{-1} \text{m}^{-1}$ ] is given by

$$\begin{aligned} \eta_0 &= \frac{2w_i^2}{\pi w_p^2 w_s^2} \frac{2\omega_i^2 d_{\text{eff}}^2 L \text{sinc}^2(\Delta k L/2)}{n_i n_p n_s c^3 \epsilon_0} \\ &= \frac{4}{\pi} \frac{\omega_i^3 \omega_p \omega_s d_{\text{eff}}^2 \text{sinc}^2(\Delta k L/2)}{(n_s \omega_s + n_p \omega_p)^2 c^4 \epsilon_0}, \end{aligned} \quad (1)$$

where  $w_i$ ,  $w_p$ , and  $w_s$  are beam radii ( $1/e^2$  intensity) at the focusing plane in the crystal;  $n_i$ ,  $n_p$ , and  $n_s$  are refractive indices; and  $\omega_i$ ,  $\omega_p$ , and  $\omega_s$  are the laser frequencies for the idler, pump, and signal beams, respectively;  $d_{\text{eff}}$  is the effective nonlinear coefficient,  $c$  is the speed of light, and  $\epsilon_0$  is the permittivity of free space. The beam diameter prefactor shown on the left-hand side of Eq. (1) can be incorporated into the conversion efficiency for optimally focused interaction, where the idler output beam is set to be confocal in the crystal ( $L = 2z_{\text{R idler}}$ ) and  $z_{\text{R}}$  is the Rayleigh length.

For a pump at 1.3 and a signal at 1.55  $\mu\text{m}$ , and thus output in the vicinity of 8  $\mu\text{m}$ ,  $\eta_0 = 2.3 \times 10^{-2} \text{W}^{-1} \text{m}^{-1}$ . With a 19-mm-long OP GaAs crystal, and laser-diode pumps amplified to 100 and

1000 mW in appropriate fiber amplifiers, the output power would be  $43 \mu\text{W}$ , suitable for a variety of sensitive spectroscopic techniques. The utility of such a source is further enhanced by the possibilities for broad wavelength tuning. For example, with pump lasers tunable over 40 nm, the output is tunable over  $0.35 \mu\text{m}$  in a single QPM grating. With multiple QPM gratings on a single chip<sup>11</sup> or a fanned QPM grating, the QPM range is readily extended to cover whatever tuning range is available from the diode pump lasers and can be tuned over as much as  $2.5 \mu\text{m}$  from 7 to  $9.5 \mu\text{m}$ . In this Letter we report on a first step in the direction of such a device, where pumps of 2.3 and 555 mW, narrowly tunable around 1.307 and  $1.567 \mu\text{m}$ , produce outputs and tuning behavior consistent with that expected from these model predictions.

We fabricated the OP GaAs crystals by first growing a thin orientation template by molecular beam epitaxy, followed by growth of a thick epitaxial GaAs layer by HVPE, as described elsewhere.<sup>12</sup> It has been shown that OP GaAs devices can be grown with good quality up to  $500\text{-}\mu\text{m}$  thickness and 20-mm length.<sup>13</sup> The present results were obtained in a device with length 19 mm, width 5 mm, thickness  $0.5 \text{ mm}$ , and grating period  $26.3 \mu\text{m}$ . A fraction of the domains ( $f \approx 0.1$ ) has an orientation that is the opposite of the nominal orientation because of growth defects. This fraction was estimated from analysis of stain-etched cross sections and the morphology of the top surface of the crystal. No significant deviation from the ideal 50% duty cycle of the QPM period was observed in the device. The input and output facets of the device were optically polished parallel within  $1^\circ$  to the  $\{110\}$ -oriented domain walls.

Figure 1 shows the experimental setup. A fiber-coupled cw distributed-feedback (DFB) laser diode (Mitsubishi Electric FU-45SDF-3) was used as a pump source. Temperature control provided wavelength tuning from 1.306 to  $1.314 \mu\text{m}$ . The pump power was wavelength dependent and ranged from 1.5 to 3.3 mW. The signal beam was generated with a cw external-cavity diode laser (DL) (New Focus Velocity 6328) that was tunable from 1.510 to  $1.580 \mu\text{m}$ , coupled to a polarization-maintaining (PM) Er-doped fiber amplifier (EDFA; IPG EAD-2-C-PM). The combined source provided high power within the Er gain band and was tuned from 1.535 to  $1.570 \mu\text{m}$  to provide  $\sim 1\text{-W}$  cw power. The polarizations of the pump and signal were set with a polarization controller and the polarization-maintaining fiber, respectively. At the sample, the signal beam was polarized parallel to the  $[100]$  growth direction of the GaAs layer, with the pump beam perpendicular to it, resulting in a nonlinear coefficient  $d_{\text{eff}} = (2/\pi)d_{14}$  (GaAs).

The pump and signal beams were focused into the OP GaAs device by lenses  $L_1$  ( $f = 300 \text{ mm}$ ) and  $L_2$  ( $f = 200 \text{ mm}$ ), respectively, and combined into coaxial beam paths parallel to the QPM grating in the device. Both beams were focused at the middle of the GaAs crystal. Beam radii ( $1/e^2$  intensity) of  $w_0 = 130 \pm 5$  and  $290 \pm 5 \mu\text{m}$  were measured for the pump and signal beam, respectively, somewhat

looser than the 115 and  $127 \mu\text{m}$  that would have led to optimum efficiency. The  $500\text{-}\mu\text{m}$  thickness of the crystal permitted easy alignment and clipping-free propagation of all three beams in the device. Two ZnSe lenses ( $f = 50 \text{ mm}$ ) focused the idler beam into a cooled mercury cadmium telluride (MCT) detector (Kolmar Technologies KMVP9-0.5). We inserted a Ge filter before the detector to block the near-IR beams and pass the idler radiation.

Optical losses were estimated by measurement of the transmission of the pump and signal beams through the HVPE layer. Fresnel losses at the uncoated facets were calculated from literature data on GaAs dispersion.<sup>14</sup> Multiple reflections were also taken into account. At the pump ( $\lambda = 1.319 \mu\text{m}$ ) and signal ( $\lambda = 1.560 \mu\text{m}$ ) wavelengths, the loss coefficient  $\alpha$  was found to be  $0.058$  and  $0.034 \text{ cm}^{-1}$  in the QPM grating patterned region, respectively, compared with  $0.033$  and  $0.02 \text{ cm}^{-1}$  in the unpatterned region next to the grating, respectively. In other samples, losses as low as  $0.025 \text{ cm}^{-1}$  even at  $1.06 \mu\text{m}$  were measured in unpatterned HVPE samples. The cause of the sample-to-sample variability, and whether the losses (and the difference between patterned and unpatterned regions of the HVPE grown film) are due to absorption or scatter are not yet clear and are currently under study. We note that these loss values at the pump and signal wavelengths, at the vicinity of the absorption edge, are significantly lower than those previously reported for bulk-grown GaAs wafers.<sup>15</sup> HVPE growth can have very low background doping,  $\sim 2\text{--}5 \times 10^{13} \text{ cm}^{-3}$ ,<sup>16,17</sup> resulting in lower absorption compared with higher doping levels in compensated semi-insulating bulk growth.<sup>18</sup> At higher wavelengths of the idler beam a free carrier absorption mechanism dominates and should be negligible in undoped HVPE, molecular beam epitaxy, films, and bulk-grown semi-insulating films with carrier concentrations below  $10^{15} \text{ cm}^{-3}$ .<sup>19</sup>

To evaluate the phase-matching conditions in the device we recorded the wavelength-tuning curve of the

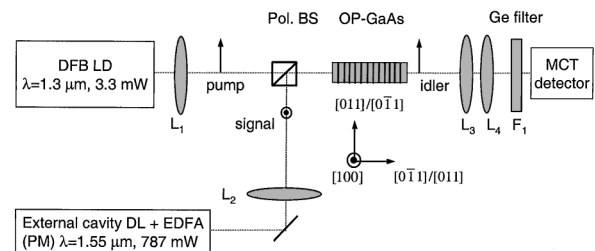


Fig. 1. Experimental setup: The pump source ( $1.3 \mu\text{m}$ , 3.3 mW) is mixed with a signal source ( $1.55 \mu\text{m}$ , 0.79 W) to generate idler wavelength radiation ( $7.9 \mu\text{m}$ , 38 nW). The polarization of the three interacting beams relative to the crystal lattice are indicated. The pump and signal are combined with a polarizing beam splitter. Lenses  $L_1$  ( $f = 300 \text{ mm}$ ) and  $L_2$  ( $f = 200 \text{ mm}$ ) are used for beam focusing into the device. ZnSe lenses  $L_3$  and  $L_4$ , with  $f = 50 \text{ mm}$ , focus the idler beam into the detector. A Ge filter,  $F_1$ , blocks the 1.3- and  $1.55\text{-}\mu\text{m}$  radiation from reaching the detector. Other abbreviations defined in text.

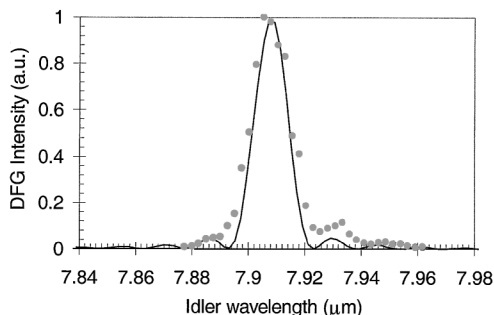


Fig. 2. Measured DFG relative intensity in OP-GaAs versus idler wavelength ( $\bullet$ ). The predicted shape of the tuning curve is shown for comparison (solid curve). The theoretical curve was slightly shifted in wavelength to coincide with experimental DFG peak location.

idler radiation by scanning the signal wavelength while keeping the pump wavelength fixed. Figure 2 shows the relative idler power versus wavelength. The predicted curve in the figure was calculated from literature data on GaAs dispersion,<sup>14</sup> and we fitted it to the experiment by slightly shifting the theoretical tuning curve to coincide spectrally with experimental data and scaling it to equal height. The peak of this tuning curve occurs at pump and signal wavelengths of  $\lambda = 1.3077$  and  $1.5669 \mu\text{m}$  respectively, resulting in an idler peak wavelength of  $\lambda = 7.905 \mu\text{m}$ . The tuning curve FWHM was found to be  $2.4 \text{ cm}^{-1}$ , close to the predicted value of  $2.16 \text{ cm}^{-1}$ . The good agreement between measured and predicted width for the nearly 2-cm-long crystal demonstrates the excellent uniformity of the material.

The theoretically expected idler output power was calculated in the near-field undepleted-pump approximation, accounting for Fresnel reflections,<sup>7,10</sup> to be  $0.1 \mu\text{W}$ , for external (internal) pump and signal powers of 3.3 (2.3) and 787 (555) mW. In this calculation we used a value of the nonlinear coefficient  $d_{14}(\text{GaAs}) = 90 \text{ pm/V}$  from a  $\text{CO}_2$  laser doubling experiment<sup>12</sup> at  $10.6\text{-}\mu\text{m}$  fundamental wavelength and scaled it via Miller's rule<sup>20</sup> to the specific wavelengths in our DFG interaction, obtaining a value of  $d_{14}(\text{GaAs}) = 104.5 \text{ pm/V}$ . We also accounted for the fraction of missing domains  $f \approx 0.1$ , which results in a reduction of the conversion efficiency  $\eta$  expressed by<sup>9</sup>  $\eta_{\text{miss rev}} = (1-2f)^2 = 0.64$ . The experimentally observed idler power was  $38 \text{ nW}$ , 2.8 times smaller than the theoretical value, reasonable given possible nonideal focusing and beam overlap in the crystal.

In conclusion, we have demonstrated generation of mid-IR radiation in all-epitaxially grown OP GaAs with length and aperture useful for bulk nonlinear interactions. The consistency between theoretical predictions and experiment for idler power and phase-matching tuning bandwidth indicates that the broadly tunable ( $2.5\text{-}\mu\text{m}$ ), narrow-linewidth (1-MHz), moderate output power ( $40\text{-}\mu\text{m}$ ) mid-IR sources for precision spectroscopy discussed at the beginning of this Letter can be based on readily available commercial components and a suitable OP GaAs crystal. We are currently working to demonstrate such a device.

This research is sponsored by U.S. Air Force Office of Scientific Research/U.S. Air Force Material Command grant F49620-99-1-0270, by U.S. Air Force Office of Scientific Research grant F49620-01-1-0428, by Defense Advanced Research Projects Agency grant MDA972-00-1-0024 through a subcontract with the University of New Mexico Optoelectronic Materials Center, and by Sandia National Laboratories through a U.S. Department of Energy prime contract. T. Skauli is permanently affiliated with the Norwegian Defense Research Establishment, which supported this work. O. Levi's e-mail address is levi@snow.stanford.edu.

## References

1. K. W. Aniolek, P. E. Powers, T. J. Kulp, B. A. Richman, and S. E. Bisson, *Chem. Phys. Lett.* **302**, 555 (1999).
2. L. A. Gordon, R. C. Eckardt, and R. L. Byer, *Proc. SPIE* **2145**, 316 (1994).
3. L. Becouarn, E. Lallier, M. Brevignon, and J. Lehoux, *Opt. Lett.* **23**, 1508 (1998).
4. E. U. Rafailov, P. Loza-Alvarez, C. T. A. Brown, W. Sibbett, R. M. De La Rue, P. Miller, D. A. Yanson, J. S. Roberts, and P. A. Houston, *Opt. Lett.* **26**, 1984 (2001).
5. C. B. Ebert, L. A. Eyres, M. M. Fejer, and J. S. Harris, Jr., *J. Cryst. Growth* **201**, 187 (1999).
6. S. Koh, T. Kondo, Y. Shiraki, and R. Ito, *J. Cryst. Growth* **227**, 183 (2001).
7. D. Zheng, L. A. Gordon, Y. S. Wu, R. S. Feigelson, M. M. Fejer, R. L. Byer, and K. L. Vodopyanov, *Opt. Lett.* **23**, 1010 (1998).
8. E. Lallier, L. Becouarn, M. Brevignon, and J. Lehoux, *Electron. Lett.* **34**, 1609 (1998).
9. M. M. Fejer, G. A. Magel, D. H. Jundt, and R. L. Byer, *IEEE J. Quantum Electron.* **QE-28**, 2631 (1992).
10. R. L. Byer, in *Nonlinear Optics*, P. G. Harper and B. S. Wherrett, eds. (Academic, London, 1977), Chap. 2, 47–160.
11. L. E. Myers, R. C. Eckardt, M. M. Fejer, R. L. Byer, and W. R. Bosenberg, *Opt. Lett.* **21**, 591 (1996).
12. L. A. Eyres, P. J. Tourreau, T. J. Pinguet, C. B. Ebert, J. S. Harris, M. M. Fejer, L. Becouarn, B. Gerard, and E. Lallier, *Appl. Phys. Lett.* **79**, 904 (2001).
13. T. J. Pinguet, O. Levi, T. Skauli, L. A. Eyres, L. Scacabarozzi, M. M. Fejer, J. S. Harris, Jr., T. J. Kulp, S. Bisson, B. Gerard, L. Becouarn, and E. Lallier, in *Conference on Lasers and Electro-Optics (CLEO)*, Vol. 56 of OSA Trends in Optics and Photonics Series (Optical Society of America, Washington, D.C., 2001), p. 138.
14. A. N. Pikhtin and A. D. Yas'kov, *Sov. Phys. Semicon.* **12**, 622 (1978).
15. S. R. Johnson and T. Tiedje, *J. Appl. Phys.* **78**, 5609 (1995).
16. C. M. Wolfe, G. E. Stillman, and W. T. Lindley, *J. Appl. Phys.* **41**, 3088 (1970).
17. G. E. Stillman and C. M. Wolfe, *Thin Solid Films* **31**, 69 (1976).
18. T. R. AuCoin and R. O. Savage, in *GaAs Technology*, D. K. Ferry, ed. (Sams, Indianapolis, Ind., 1985), Chap. 2, pp. 47–78.
19. J. S. Blackmore, *J. Appl. Phys.* **53**, R123 (1982).
20. M. M. Choy and R. L. Byer, *Phys. Rev. B* **14**, 1693 (1976).